Multicomponent Mass Transfer in Turbulent Flow

G. L. VON BEHREN, W. O. JONES, and D. T. WASAN

Department of Chemical Engineering
Illinois Institute of Technology, Chicago, Illinois 60616

A general treatment of entry region multicomponent mass transfer between a fully developed turbulent flow and a smooth pipe wall has been developed from a basis first derived by Toor.

The coupled multicomponent equations were reduced to an equivalent binary system by the method of undetermined constants. Numerical solutions for a forced convection, binary diffusion system involving gas-phase, nonequimolal diffusion were applied to a ternary system. These solutions have been found to compare well with these authors entry region mass transfer data on a ternary acetone-methanol-air mixture and with the earlier analogy theories derived for the case of an infinitely long test section.

We conclude that there is a significant interaction in some multicomponent systems, enough that the binary theory can not be satisfactorily applied in the design of multicomponent mass transfer systems.

Gas-phase mass transport in multicomponent mixtures in turbulent flow is of considerable industrial interest. Development of theoretical models using momentum mass transfer analogy theory (confined to the regions of fully developed convective mass transfer) to describe any multicomponent system, especially ternary systems, was published by Toor and Sebulsky (*5*) in a two-part series of papers. Three models were proposed: film, modified Prandtl-Taylor, and Chilton-Colburn. The Chilton-Colburn analogy was modified by Carleton and Oxley (*1*) by correcting the Sherwood number to reflect the effect of a large molecular weight change across the diffusion barrier. Toor later published two methods for linearizing the diffusion equations in a multicomponent system to a set of equivalent binary equations. His matrix technique is adaptable to all multicomponent systems (*7*), while a determinant solution is found useful in the ternary case (*6*) because of its relative simplicity. Stewart and Prober (*4*) also derived a matrix technique for multicomponent systems about the same time as Toor, but Toor, Seshadri, and Arnold (*8*) showed the methods to be equivalent. Cullinan (*2*) and Wills (*15*) made similar simplifications with multicomponent liquid systems.

It is the purpose of this paper to develop and test a multicomponent entry region mass transfer theory in turbulent flow by using extensively the developments of Toor's equivalent binary system. The fully developed region is also studied to verify the limit of the entry region equations. Numerical solutions for a forced convection ternary system involving gas-phase, nonequimolar diffusion have been applied to the entry region of a fully developed turbulent pipe flow.

THEORETICAL ANALYSIS

The determinant method of Toor (*6*) is used to uncouple the multicomponent time-averaged equations of convective diffusion which can be described by the equation

$$\nabla\, (\underline{V}\, C_i) = \nabla\, [\Sigma_j\, (D + \epsilon)_{ij}\, \nabla\, C_j] \tag{1}$$

This yields a set of $n - 1$ independent equations coupled by the cross-diffusion coefficients $(D + \epsilon)_{ij}$ where $i \neq j$. Equation (1) has been solved by Toor for the ternary case where the eddy diffusivity is unimportant. This method is now extended to include both molecular and turbulent diffusivities.

By summing Equation (1) over the $n - 1$ independent species and by multiplying by the undetermined constant s_i, Equation (2) is obtained:

$$\nabla\, \underline{V}\, (\Sigma_i\, s_i\, C_i) = \nabla\, [\Sigma_i\, \Sigma_j\, s_i\, (D + \epsilon)_{ij}\, \nabla\, C_j] \tag{2}$$

Equation (2) will reduce to a binary form if the s_i's are chosen such that

$$(D + \epsilon)_k\, \Sigma_i\, s_i\, C_i = \Sigma_i\, \Sigma_j\, s_i\, (D + \epsilon)_{ij}\, \nabla\, C_j \tag{3}$$

where the $(D + \epsilon)_{ij}$ represent the ternary diffusion coefficients, and $(D + \epsilon)_k$ is the root of the equation. The eddy viscosity ϵ_{ij}, appearing in Equation (3), is a function of position; thus, s_i and $(D + \epsilon)_k$ are also functions of position. Equation (3), therefore, is valid only if it is assumed that the differential Equation (2) can be broken into discrete small intervals for solution.

For clarity, the notation D_k will represent $(D + \epsilon)_k$, the total diffusivity. If an additional subscript is added to the constants s_i such that s_{ik} represents the constant corresponding to a function of the root D_k, then Equation (3) can be rearranged to equate the coefficients of the concentrations, yielding

$$\Sigma_i\, s_{ik}\, (D + \epsilon)_{ij} - s_{jk} D_k = 0 \tag{4}$$

If it is further assumed that the s_{ii} can be set equal to one, the remaining s_{ik} can be found.

By assuming that the eddy diffusivity is independent of the particular components involved, $\epsilon_{ij} = \epsilon$, the expression for the constant s_{ij} is

$$s_{ik} = \frac{D_k - (D_{kk} + \epsilon)}{(D_{ik} + \epsilon)} \tag{5}$$

Correspondence concerning this paper should be addressed to D. T. Wasan. G. L. von Behren is with the American Oil Company, Whiting, Indiana 46394. W. O. Jones is with the Dow Chemical Company, Midland, Michigan 48640.

where

$$2D_k = (D_{11} + D_{22} + 2\epsilon) \pm \sqrt{(D_{11} - D_{22})^2 + 4(D_{12} + \epsilon)(D_{21} + \epsilon)} \quad (6)$$

Now, if an equivalent binary concentration is defined as

$$\psi_k = \Sigma_i \, s_{ik} \, C_i, \qquad k = 1, \ldots, n - 1 \quad (7)$$

Equation (2) may be uncoupled by substituting Equation (3) into (2) and by inserting Equation (7), yielding

$$\nabla \, (\underline{V} \, \psi_k) = \nabla \, (D_k \, \nabla \, \psi_k) \quad (8)$$

the equivalent binary equation. For a ternary system, two equivalent binary equations are necessary to define the system.

For the case of constant total concentration, Equation (7) may be modified to

$$\psi_k = \Sigma_i \, s_{ik} \, W_i \quad (9)$$

and Equation (8) becomes

$$\underline{V} \cdot \nabla \, \psi_k = \nabla \, (D_k \, \nabla \, \psi_k) \quad (10)$$

This general steady state forced diffusion convection can be simplified for the case studied here. It is assumed that diffusion in the axial direction is insignificant and may be neglected, diffusion in θ direction is negligible, fluid enters the test section with a fully developed velocity profile, and the mass transfer does not contribute to any change in the time averaged velocity distribution as fluid travels downstream.

In the mass transfer processes such as evaporation, the transfer mechanism can be approximated as a diffusion of solute through a gas which exhibits no net transfer in the direction of the solute transfer. Rigorously, the flux of the nondiffusing species is zero only at the wall, but it is assumed here that it is zero at every radial position in the pipe. This has been shown to be a reasonable assumption at ordinary mass transfer rates (*9*, *14*). The resulting crossflow velocity can be found from

$$V_r = -\frac{D_k}{1 - \psi_k} \left(\frac{\partial \psi_k}{\partial r} \right) \quad (11)$$

The diffusion convection Equation (10) becomes

$$V_z \frac{\partial \psi_k}{\partial z} = \frac{1}{r} \frac{\partial}{\partial r} \left[D_k \, r \frac{\partial \psi_k}{\partial r} \right] + \frac{D_k}{1 - \psi_k} \left(\frac{\partial \psi_k}{\partial r} \right)^2 \quad (12)$$

Since D_k contains the eddy diffusivity, it is thus a function of position. Equation (12), then, is a nonlinear second-order equation. The boundary conditions for this problem are:

1. $\psi = \psi_0$ at $z = 0$, at the test section inlet, for all $r > 0$; that is, the concentration of the entering gas stream is constant.

2. $\psi = \psi_w$ at $r = R$, at the pipe wall; for all $z > 0$; that is, the wall concentration is constant at all downstream distances.

3. $\dfrac{\partial \psi}{\partial r} = 0$ at $r = 0$, the pipe center line, for all z.

There is no concentration gradient at the axis of the tube, and the equivalent concentration profile is symmetric about the radial axis.

Solution of the equivalent diffusion convection equation is accomplished after reducing Equation (12) to a dimensionless form. A complete derivation of the quantities has been developed elsewhere (*3*, *14*), and only a basic summary and explanation of the deviations from that derivation will be mentioned here.

Although numerous velocity and eddy viscosity correlations are available in the literature, the original Wasan-Tien-Wilke relationship as corrected by Jones (*3*) for the wall region and the von Karman turbulent core relation has been chosen. For the wall region

$$V_z{}^+ = U^+ = y^+ - 1.098 \times 10^{-4}(y^+)^4 + 3.30 \times 10^{-6}(y^+)^5 \quad (13)$$

and

$$\frac{\epsilon}{\nu} = \frac{4.39 \times 10^{-4}(y^+)^3 - 16.5 \times 10^{-6}(y^+)^4}{1 - 4.39 \times 10^{-4}(y^+)^3 + 16.5 \times 10^{-6}(y^+)^4} \quad (14)$$

while for the turbulent core

$$V_z{}^+ = U^+ = 2.5 \ln y^+ + 5.5 \quad (15)$$

and

$$\frac{\epsilon}{\nu} = \frac{y^+ \, (1 - y^*)}{2.5} - 1.0 \quad (16)$$

In accordance with the available experimental work that has shown eddy diffusivity to pass through a maximum and reach a constant value, the eddy diffusivities between $y^* = 0.8$ and $y^* = 1.0$ are assumed to have the constant value corresponding to $y^* = 0.8$. To make the diffusion convection equation dimensionless, the following must be defined:

$$y^* = \frac{y}{R} \quad \text{and} \quad y^+ = \frac{y^* R U_\tau}{\nu} \quad (17)$$

where U_τ, the friction velocity, is

$$U_\tau = \sqrt{\frac{\tau_w g_c}{\rho}} = \overline{U} \sqrt{f/2} = \overline{V}_z \sqrt{f/2} \quad (18)$$

and $\overline{U}$ is the mean axial velocity.

The dimensionless equivalent binary concentration is, with the subscript omitted for clarity

$$\psi^+ = \frac{\psi - \psi_0}{\psi_w - \psi_0} \quad (19)$$

All dimensionless quantities are substituted into Equation (12), and a numerical approach is used to solve this equation. A change in variables as employed by Wasan et al. (*14*) is used to expand the wall region, and Equation (12) is solved by finite difference, with the Dufort-Frankel method used. The computer program is available elsewhere (*10*). Output from the programs is in the form of dimensionless equivalent binary concentration profiles as defined by Equation (9), average equivalent concentrations, and binary equivalent Stanton numbers.

In order to recover the actual component concentration profiles or Stanton numbers in a ternary mixture from the equivalent binary solution, the s_i previously determined must be used again.

For a ternary mixture

$$\psi_1 = W_1 + s_{21} \, W_2 \quad (20)$$

and

$$\psi_2 = s_{12} \, W_1 + W_2 \quad (21)$$

Equations (20) and (21) are a set of two linear equations which may be solved by determinants yielding

$$W_k = \frac{s_{jj}\psi_k - s_{jk}\psi_j}{|s_k|} \quad (22)$$

where $|s_k|$ is the second-order determinant of the constants s_{ik}. In general, matrix methods as used by Toor (*6*) and Stewart and Prober (*4*) may be employed for solving the multicomponent mass transfer problem. For the cases studied experimentally here, where the center line concentrations are negligible, the dimensionless weight fraction can be expressed as

$$W_k{}^+ = \frac{s_{jj}(\psi_{kw}\ \psi_k{}^+) - s_{jk}(\psi_{jw}\ \psi_j{}^+)}{s_{jj}(\psi_{kw}) - s_{jk}(\psi_{jw})} \qquad (23)$$

The equivalent binary Stanton numbers generated may be converted to the actual multicomponent form by utilizing the definition of the equivalent binary flux, where

$$\eta_k = k_k\ \Delta\ \psi_k = \Sigma_i\ s_{ik}\ N_i, \quad k = 1, \ldots, n-1 \qquad (24)$$

is defined similarly to the equivalent concentration as given by Equation (19). Solving Equation (24) for a particular $\underline{N_i}$ and substituting into the binary flux equation, one obtains

$$\underline{N_i} = \frac{\Sigma_j \Sigma_k S_{ik} s_{jk} k_k}{|s_k|}\ \Delta\ C_j \qquad (25)$$

or

$$\underline{N_i} = \Sigma_j k_{ij} \Delta C_j \qquad (26)$$

where

$$k_{ij} = \frac{\Sigma_k S_{ij} s_{jk} k_k}{|s_k|} \qquad (27)$$

The k_{ii} are the main multicomponent mass transfer coefficients and k_{ij} $(i \neq j)$ the cross coefficients.

Defining the multicomponent Stanton number similar to the binary Stanton coefficient, one gets

$$N_{St_{ik}} = \frac{k_{ik}}{\overline{U}} \qquad (28)$$

where the mass transfer coefficients k_{ij} are defined from Equation (27). It is to be noted that when $i \neq j$ in Equation (27), the resulting Stanton number is a measure of the interaction effect between components. A comparison between the St_{ii} and St_{ij} $(i \neq j)$ would indicate the relative importance of the interactions.

EXPERIMENTAL APPARATUS AND PROCEDURE

The experimental apparatus was designed to study vaporization of a constantly evaporating binary liquid mixture from the surface of a horizontal porous pipe into a turbulent air stream.

The integral component of the equipment, shown in Figure 1, is the porous ceramic pipe used as the inner annulus of the test section and constructed from extra fine, fused alumina grains of a uniform size and structure. Its porosity is defined in terms of pore diameter and permeability. Having a maximum pore diameter of 40 μ, its permeability is 0 to 1 cu. ft. of 70°F. air/min./sq.ft. of surface area. It has an inside diameter of 6 in. and a wall thickness of 0.5 in. The outer annular shell is an 8-in. aluminum pipe cut to a length of 35.75 in.

Thermocouples constructed of 30 gauge copper constantan wire were placed at thirty positions throughout the 3-ft. long porous pipe. This series of thermocouples records both axial and radial temperature profiles on the inside, middle, and outside of the test section. Surface thermocouples did not actually lie on the surface but were placed as close to the surface as possible, and a thin layer of Silastic cement covered the weld. Small holes were drilled into the test section at aspect ratios of 0.25, 2, 4, and 5.75 for thermocouple wells.

To hold the cylinders together, flanges with two precision machined recesses were designed for each end face. These flanges have an 11 in. O.D., 6 in. I.D., and an initial circular recess diameter of 8.6 in. cut 0.25 in. deep. To house the porous cylinder another 0.25 in. recess 6.5 in. in diameter was cut. Both shells of the annulus were force fitted to the flanges and sealed with Silastic. Restraining rods maintained the snug fit. Four holes at 90 deg. intervals were drilled into the flanges for mounting to the developing and exit sections.

Circulation within the test section was necessary to achieve a uniform temperature profile and to prevent localized cooling in areas away from the exit ports. Seven 0.25 in. pipe thread holes were drilled and tapped, four along the bottom and three along the top, and four 0.125 in. pipe thread holes were added along the top for exit and entry circulation ports. Pipe manifolds were constructed in a staggered tee arrangement between ports to assist in obtaining uniformity of flow into the test section. The flow of liquid to the surface of the porous pipe was much larger than the quantity of liquid evaporated, and hence the surface was continuously renewed with new liquid. Draw off from the bottom ports is fed through a small centrifugal pump and recirculated to a fresh feed tee, through a 5,000 w. electrical heater to supply heat for warming, and refed to the top ports.

The exit gas mixture was exhausted to the atmosphere after passing through a conical diffuser to prevent back pressure effects.

Data points were collected from a pitot tube connected to a vertical and horizontal gear train mounted on the pipe to the rear of the test section. The tip of the impact tube was filed to an outside diameter of 0.4 mm. or 0.0025 in. The pitot tube was connected to an inclined tube micromanometer (range: 0 to 0.2 in. of water) for velocity readings. Concentration readings were taken isokinetically from the impact side of the pitot tube by using a gas chromatograph to analyze the sample. Temperatures at any point within the test section were measured by using 30 gauge copper constantan thermocouples mounted on each side and immediately to the rear of the tip of the impact side of the pitot tube.

Vaporization runs were made at Reynolds numbers of 20,000 and 40,000 by using an acetone-methanol mixture for the wall fluids. All runs were made at a wall temperature of 80°F. and atmospheric pressure. Further details on the equipment and procedure used can be found elsewhere (*10*).

Equipment performance was checked to verify the assumption of fully developed symmetrical flow by comparing data with semitheoretical velocity profiles. The velocity profile in the test section was fully developed, and it did not significantly deviate from the velocity conditions under no mass transfer. Details of this comparison are available elsewhere (*10*).

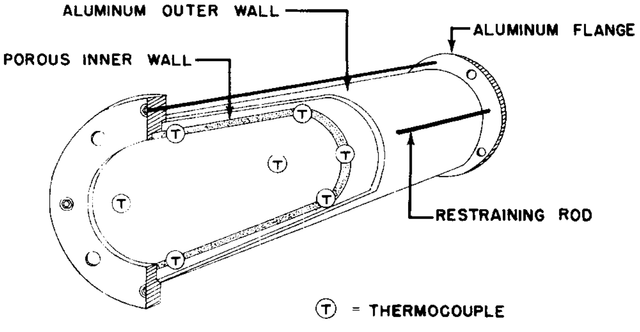

Fig. 1. Auxiliary cutaway view of the test section.

RESULTS AND DISCUSSION

The entry region theory for turbulent pipe flow was compared with experimental data for a ternary system. Since the acetone-methanol-air system chosen showed only mild interaction, a second ternary system of acetone-benzene-helium was theoretically studied to observe the effects of a strongly interacting system. As a verification of the theoretical analysis, the earlier analogy theories of Toor and Sebulsky (5) for infinitely long sections were compared with Stanton number plots. After confidence was established in the preliminary performance of the apparatus, a series of computer runs was made to simulate the first experimental system studied. Figure 2 shows the set of constants s_{ik} and the determinant $|s_k|$ necessary to set up the boundary conditions for the equivalent binary equation at a Reynolds number of 20,000. These coefficients are applied to the equivalent binary concentration profiles generated by the entry region programs to obtain the actual multicomponent concentration profiles.

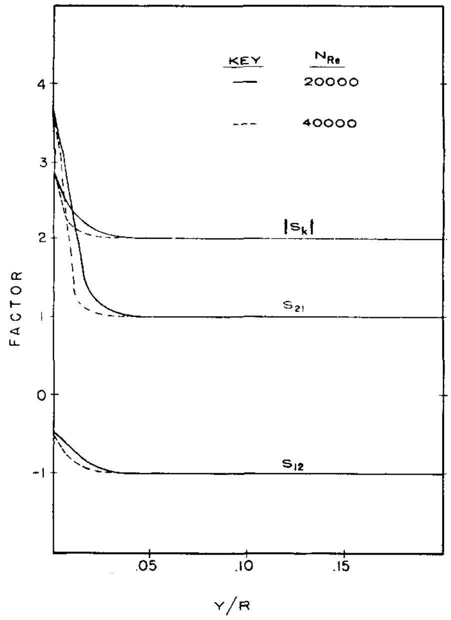

Fig. 2. Multicomponent interaction factors for acetone-methanol-air system.

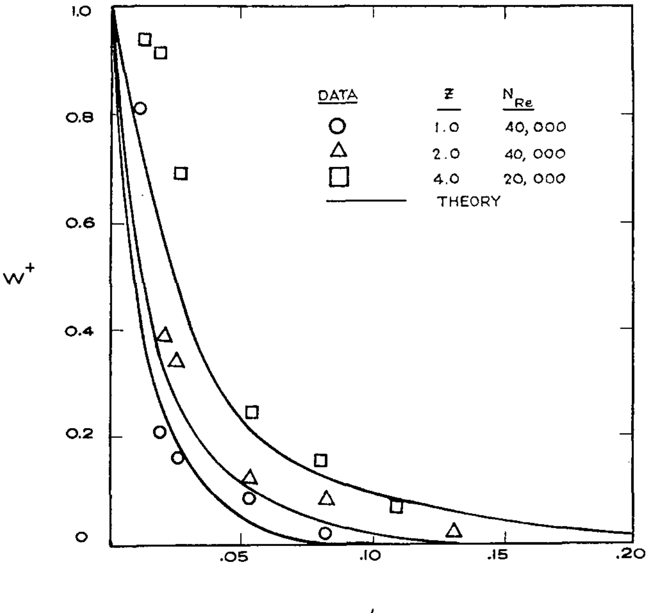

Fig. 3. Comparison of experimental data with the predicted acetone multicomponent profiles for $N_{Sc} = 1.1$.

TABLE 1. EXPERIMENTAL CONCENTRATION PROFILES FOR THE ACETONE-METHANOL-AIR SYSTEM

Aspect ratio = 4 Reynolds number = 20,000

y^*	X_{Ac}	W_{Ac}	W^+
0.0131	0.175	0.298	0.954
0.0197	0.170	0.290	0.930
0.0263	0.122	0.217	0.695
0.0526	0.040	0.077	0.247
0.0789	0.028	0.054	0.175
0.131	0.011	0.020	0.064

$W^+ = 0.051$

Aspect ratio = 1 Reynolds number = 40,000

y^*	X_{Ac}	W_{Ac}	W^+
0.0131	0.205	0.34	0.81
0.0197	0.043	0.0824	0.196
0.0263	0.035	0.0676	0.161
0.0526	0.0205	0.0401	0.096
0.0789	0.008	0.0139	0.033

$\overline{W}^+ = 0.0182$

Aspect ratio = 2.0

y^*	X_{Ac}	W_{Ac}	W^+
0.0197	0.097	0.162	0.386
0.0263	0.085	0.145	0.345
0.0526	0.029	0.056	0.133
0.0789	0.025	0.049	0.1-7
0.1310	0.008	0.016	0.038
0.262	0.002	0.004	0.009

$W_w = 0.42$ $\overline{W}^+ = 0.0299$

Aspect ratios of 2.0 and 4.0 were experimentally studied at a 20,000 Reynolds number. Average wall temperature was 80°F. with a possible deviation of ± 8°F. due to a nonuniformity of the test section porosity. The acetone multicomponent profiles* at an aspect ratio of 4.0 is shown in Figure 3. The experimental values for this Reynolds number are tabulated in Table 1. Experimental data points for an aspect ratio of 4.0 are plotted against the predicted profiles from Equation (23). The deviation of the experimental points from the calculated profile in the wall region in Figure 3 can be attributed to the fact that very small concentrations are being measured at low aspect ratios. In addition, very close to the wall, where the velocity is small and the concentration gradient is large, an extremely long interval of time is required to achieve an accurate concentration specimen by the isokinetic sampling technique. The precision of correlating pitot tube position is also a significant factor in the error analysis. The average absolute deviation in concentration from the theoretical curve at an aspect ratio of 4.0 is 7%.

A second set of traverses was taken at a Reynolds number of 40,000. The set of undetermined constants necessary to define the equivalent binary system is also plotted in Figure 2. The curves are of the same general shape as those at 20,000 but become steeper closer to the wall. This would tend to indicate that the interaction effect is more pronounced within the region very close to the wall.

The acetone multicomponent concentration profiles are shown in Figure 3. The data for these profiles are found in Table 1. At an aspect ratio of 1.0, the data scatter introduce an error of 10.2%. At an aspect ratio of 2.0, the predicted profile is lower than actually encountered, and the average deviation is 17.8%. The concentration profile taken at an aspect ratio of 4.0 is not plotted because of wetting problems caused by clogging of the pores in the test section by grit which bypassed the feed filter.

To further compare the proposed multicomponent theory, Stanton numbers were plotted to compare limiting values with earlier analogy theories.

Stanton numbers as defined by Equation (28) are plotted for the acetone and methanol species of a ternary mix-

---

* The phrase *multicomponent profile* refers to a profile obtained from a ternary system; *binary profile* refers to a profile obtained from a binary system.

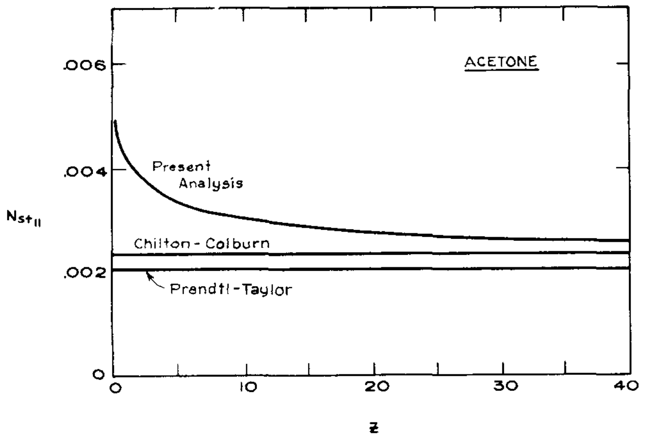

Fig. 4. Axial Stanton number profile compared with analogy theories for the acetone component of the experimental system: $N_{Re} = 40{,}000$; $N_{Sc} = 1.1$.

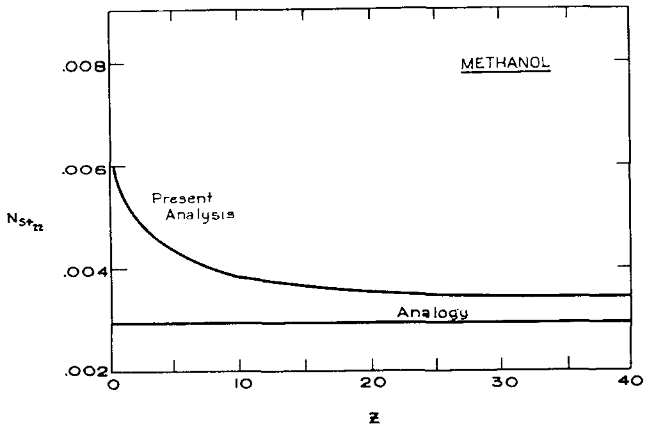

Fig. 5. Axial Stanton number profile compared with analogy theories for the methanol component of the experimental system: $N_{Re} = 40{,}000$; $N_{Sc} = 0.94$.

ture as a function of downstream distance. This allows the asymptotic value for the Stanton number to be determined from the present theory and a direct comparison with analogy theory values to be made. Figure 4 shows the variation of the local acetone Stanton number with downstream distance. The present analysis is compared with the Chilton-Colburn and Prandtl-Taylor analogies at a Reynolds number of 40,000. The Prandtl-Taylor analogy predicts a value which is 18.8% lower than the asymptotic value of the entry region theory, while the Chilton-Colburn value is 13.5% lower than the proposed theory. The comparison between the predicted methanol entry region profile with analogy values is shown for a Reynolds number of 40,000 in Figure 5. The asymptotic value predicted by the present analysis is 12.4% higher than all the analogy values. It is of interest to note that there is no deviation between the various analogy values for the methanol species as there was for the acetone component. This is due to the diluteness of the methanol species in the system studied.

The Carleton-Oxley (*1*) molecular weight correction was applied to the multicomponent Chilton-Colburn analogy and tested against Toor and Sebulsky's binary runs. It showed no significant improvement in their data. For the case studied above, the factor overcorrected and predicted an analogy value 72% lower than the present analysis, significantly differing from both the present theory as well as the other analogies used here. However, qualitatively, the concept of a molecular weight correction appears to be useful in correcting the deviation from experiment, but, in the turbulent region, the effect does not appear to be of the form suggested by Carleton and Oxley based on their low Reynolds number flow data.

Equation (28) also predicts a Stanton number $N_{St_{ik}}$, where $i \neq k$. This cross Stanton number is a measure of the interaction effects. $N_{St_{12}}$ describes the interaction of the acetone on the methanol. At both Reynolds numbers studied, this Stanton number is of the same order of magnitude as the main acetone Stanton number $N_{St_{11}}$. However, a comparison of $N_{St_{21}}$, the cross Stanton number that describes the effect of the methanol on the acetone, with the main Stanton number for methanol, $N_{St_{22}}$, shows that $N_{St_{21}}$ is ten times smaller than $N_{St_{22}}$. These data for a Reynolds number of 40,000 are tabulated in Table 2. This tends to indicate that there is very little effect of the methanol on the acetone, as would be expected for a dilute species.

To establish whether interactions are of any significance in the system, the corresponding acetone-air binary system was studied for a wall temperature of 80°F. at a Reynolds number of 20,000. The method developed earlier by Wasan and Wilke (*13*) and most recently by Wasan et al. (*14*) was used to simulate this system. Since the theory used in both binary and ternary cases is derived from a common basis, the resultant Stanton numbers for each system should be identical if no interactions are present. However, the binary acetone Stanton number is 18.3% higher than the main acetone multicomponent Stanton number. A second set of runs for the methanol-air binary system at an 80°F. and 20,000 Reynolds number yields a binary Stanton number which is 9.5% higher than the corresponding ternary case. This would indicate that introduction of the third component does interact, causing a change in the Stanton number.

The second multicomponent mixture studied theoretically is a benzene-acetone-helium system at 80°F. and a Reynolds number of 20,000. Toor and Sebulsky (*5*) have previously shown this system to be strongly interacting in their wetted wall data. Computer results for a ternary concentration profile in the developing region is compared with the corresponding acetone-helium binary system at the same temperature and an aspect ratio of 1.0 as shown in Figure 6. The acetone ternary profile predicts a faster development than its corresponding binary system. This comparison would tend to verify that there is a significant interaction in some multicomponent systems, enough that the binary theory cannot be satisfactorily applied.

TABLE 2. MULTICOMPONENT STANTON NUMBERS CALCULATED FROM PRESENT ANALYSIS AT A REYNOLDS NUMBER OF 40,000 FOR THE ACETONE-METHANOL-AIR SYSTEM

Z	$N_{ST_{11}}$	$N_{ST_{22}}$	$N_{ST_{12}}$	$N_{ST_{21}}$
0.0004	0.02792	0.03598	0.03211	0.00425
0.0100	0.01715	0.02225	0.02028	0.00268
0.0250	0.01176	0.01444	0.01066	0.00141
0.0500	0.00926	0.01184	0.01027	0.00136
0.1000	0.00755	0.00965	0.00832	0.00110
0.1500	0.00662	0.00848	0.00741	0.00098
0.2500	0.00585	0.00760	0.00695	0.00092
0.5000	0.00505	0.00651	0.00577	0.00076
0.7500	0.00477	0.00607	0.00515	0.00068
1.0000	0.00446	0.00575	0.00511	0.00068
2.0000	0.00394	0.00508	0.00452	0.00060
4.0000	0.00348	0.00449	0.00399	0.00053
5.0000	0.00335	0.00432	0.00389	0.00051
10.0000	0.00298	0.00386	0.00354	0.00047
20.0000	0.00276	0.00357	0.00321	0.00042

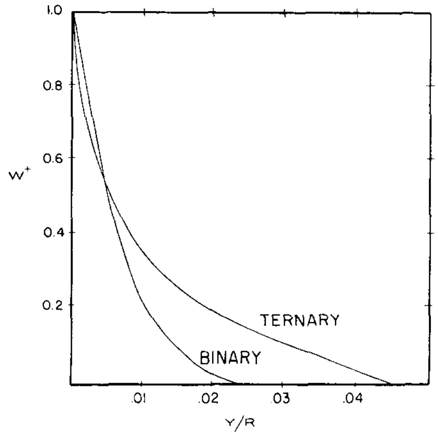

Fig. 6. Comparison of the acetone concentration profile for the multicomponent and binary system: $N_{Re} = 20{,}000$; $N_{Sc} = 1.1$; $Z = 1.0$.

CONCLUSIONS

1. At low rates of mass transfer, for a ternary system at constant Schmidt and Reynolds number, the method of Toor may be applied with the multicomponent turbulent diffusion-convection equation to find an equivalent binary system for solution. The multicomponent local Stanton numbers obtained in the entry region satisfactorily converge to an asymptotic value which correlates well with independent predictions based on analogy theory.

2. Experimental data in the form of concentration profiles for an acetone-methanol-air ternary system agree with the proposed theory within experimental limitations. Furthermore, verification of the theory with limited experimental data has also shown that there is a pronounced entry region effect. No earlier entry region data for multicomponent systems have been published in the literature.

3. Comparison of earlier analogy theories with asymptotic values of the present computer calculations of the diffusion-convection equations has shown that there is no significant difference between the multicomponent Chilton-Colburn and Prandtl-Taylor analogies for very dilute systems. However, the multicomponent Chilton-Colburn analogy agrees better with the computed results for more concentrated systems. Toor and Sebulsky had earlier proposed that only the Prandtl-Taylor version be accepted.

4. The interaction between diffusing species in a multicomponent mixture plays an important role in the design of multicomponent mass transfer systems.

ACKNOWLEDGMENT

Financial support for this study was partly provided by an American Oil Fellowship, the Institute of Gas Technology and the National Science Foundation under Grant GK-255. The authors also wish to thank the Planning and Engineering Department of the American Oil Company for technical assistance.

NOTATION

C_i = molar concentration of species i
C = total molar concentration
d = diameter of the pipe
D_k = equivalent binary diffusivity including the eddy diffusivity effect
D_{ij} = multicomponent molecular diffusivity
k_{ij} = multicomponent mass transfer coefficient based on weight fraction basis
N_i = binary flux
r = radial distance
R = radius of the tube
S_{ij}, s_{ij} = interaction constant
$U = V_z$ = axial velocity
$U^+ = V_z^+$ = dimensionless velocity $= U/U_\tau$
$\underline{V}$ = velocity vector
W_i = mass fraction of species i
W^+ = dimensionless mass fraction, $\dfrac{W_A - W_{A0}}{W_{AW} - W_{A0}}$
$\overline{W^+}$ = dimensionless average mass fraction
W_{Ac} = mass fraction of acetone
W_w = mass fraction at the wall
X_{Ac} = mole fraction of acetone
y = distance from the pipe wall
Z = aspect ratio $= z/d$
z = axial direction, axial distance

Dimensionless Groups

N_{Re} = Reynolds number $= \overline{U}\, d/\nu$
N_{Sc} = Schmidt number $= \nu/D$
N_{St_i} = binary Stanton number $= k_i/\overline{U}$
$N_{St_{ik}}$ = multicomponent Stanton number $= k_{ik}/\overline{U}$

Greek Letters

ρ = density
μ = viscosity
ν = kinematic viscosity
ϵ = eddy diffusivity
η = equivalent binary flux
ψ_4 = equivalent binary concentration
τ_w = shear stress at the wall

Subscripts

0 = incoming stream
i, j, k = species indexes
r = radial direction
w = wall value
z = axial direction

LITERATURE CITED

1. Carleton, H. E., and J. H. Oxley, *AIChE J.*, **13**, 571 (1967).
2. Cullinan, T., *Ind. Eng. Chem. Fundamentals*, **4**, 139 (1965).
3. Jones, W. O., Ph.D. thesis, Ill. Inst. Technol., Chicago (1969).
4. Stewart, W. E., and R. Prober, *Ind. Eng. Chem.*, **3**, 224 (1964).
5. Toor, H. L., and R. T. Sebulsky, *AIChE J.*, **7**, 558, 565 (1961).
6. Toor, H. L., *ibid.*, **10**, 448 (1964).
7. *Ibid.*, 460.
8. ———., C. V. Seshadri, and K. R. Arnold, *ibid.*, **11**, 746 (1965).
9. Vivian, J. E., and W. C. Behrmann, *ibid.*, 746.
10. von Behren, G. L., M.S. thesis, Ill. Inst. Technol., Chicago (1969).
11. Wasan, D. T., Ph.D. thesis, Univ. Calif., Berkeley (1965).
12. ———., and C. R. Wilke, *Intern. J. Heat Mass Transfer*, 7, 87 (1964).
13. —————., *AIChE J.*, **14**, 227 (1968).
14. Wasan, D. T., W. O. Jones, and G. L. von Behren, *ibid.*, **17**, 300 (1971).
15. Wills, G. B., *Ind. Eng. Chem. Fundamentals*, **6**, 142 (1967).

Manuscript received November 3, 1970; revision received April 30, 1971; paper accepted April 30, 1971.